Dynamic activation of distinct cytoarchitectonic areas of the human SI cortex after median nerve stimulation

Isao Hashimoto,[1,2,CA] Tomoaki Kimura,[3] Yoshinobu Iguchi,[4] Ryosuke Takino[5] and Kensuke Sekihara[6]

[1]Human Information Systems Laboratory (Tokyo Office), Kanazawa Institute of Technology, 6-7-8 Akasaka, Minato-ku, Tokyo 107-0052; [2]Department of Integrative Physiology, National Institute for Physiological Sciences, Okazaki; [3]Department of Acupuncture, Tsukuba College of Technology, Tsukuba; [4]Department of Psychophysiology, Tokyo Institute of Psychiatry, Tokyo Metropolitan Organization for Medical Research, Tokyo; [5]Department of Psychology, Shiraume Gakuen College, Tokyo; [6]Department of Electronic Systems and Engineering, Tokyo Metropolitan Institute of Technology, Tokyo, Japan

[CA,1]Corresponding Author and Address

Received 7 March 2001; accepted 11 April 2001

MEG recordings visualized non-invasively a serial mediolateral activation of the human somatosensory 3b area followed by a stationary activation of area 1 after median nerve stimulation. Somatosensory evoked fields (SEFs) were recorded over the hand area contralateral to the right median nerve stimulation at the wrist in six normal subjects. A newly developed MEG vector beamformer technique applied to the SEFs revealed two distinct sources (areas 3b and 1) in the primary somatosensory cortex (SI) during the primary N20m-P22m response in all subjects. The first source was located in area 3b, which started to move sequentially toward mediolateral direction 0.7 ms prior to the peak of N20m and ended its movement 1.4 ms after the peak with a total distance of 11.2 mm. We speculate that the movement reflects a sequential mediolateral activation of the pyramidal cells in area 3b, which is mediated by horizontal connections running parallel to the cortical surface. The second source in area 1, located 5.6 mm medial and 4.2 mm posterior to the first source, was active 1.0 ms after the N20m peak. Then, the first source became inactive and the second source was dominant. In sharp contrast with the first source, the second source was stationary. The different behavior of these two components (moving *vs* stationary) indicates independent parallel inputs to area 3b and area 1 from the thalamus. *NeuroReport* 12:1891–1897 © 2001 Lippincott Williams & Wilkins.

Key words: Area 3b; Area 1; Horizontal fibers; Median nerve; MEG vector beamformer technique; Moving source; N20m-P22m; Parallel thalamocortical inputs; Somatosensory evoked fields; Stationary source; Two overlapping sources

INTRODUCTION

It has long been considered established that N20 primary response in the somatosensory evoked potentials (SEPs) after median nerve stimulation is generated in area 3b and is approximated by a fixed dipole. However, in a recent magnetoencephalographic (MEG) study by Hashimoto *et al.* [1], it was suggested that N20m equivalent current dipole (ECD) is not stationary and moves sequentially from medial to lateral direction in area 3b. With regard to the following P22 component (corresponding to Allison's P25), it is well established that one of the generators for this component is located in the anterior crown of the postcentral gyrus in area 1 of primary somatosensory cortex (SI) [2–5]. However, there has been a considerable debate about the contribution of area 4 of primary motor cortex (M1) to this component [2,5,6]. Even if area 4 is active, co-activation of two anti-parallel dipoles, one in area 3b and another in area 4 will mutually cancel out the magnetic fields generated in respective areas.

The issue has been complicated further when source localization for the activity of a relatively wide area is to be estimated using a single dipole model. In the somatosensory hand area, the central sulcus takes a curved course resembling the inverted letter Ω [7]. The cortical activation after median nerve stimulation can be seen as an extended sheet of dipoles and the ECD model gives us an estimate of the center of gravity of this activity. Given that the lateral part of the inverted Ω receives projection from the median nerve, the center of gravity of this activation can well be in the precentral wall (area 4) instead of in the postcentral wall (area 3b) [8].

The MEG vector beamformer technique recently developed by Sekihara *et al.* [9,10] provides us with a unique tool for the analysis of multiple sources located nearby, which are activated simultaneously and/or successively. In order to overcome the above difficulties in previous studies, the N20m-P22m response for stimulation of median nerve was characterized by applying the beamformer technique. We found that two distinct sources, one in area 3b and another in area 1, were sequentially and simulta-

neously active during N20m-P22m response and even during a single peaked N20m response. The results using a single dipole model were reported previously [1]. However, the study was confined to ECD estimations around the peak of N20m and the ECDs for a later part of N20m including the superimposed P22m were difficult to localize. In fact, we have often failed to estimate the ECD localizations with the single dipole model.

MATERIALS AND METHODS

Six healthy adults (two females, four males; ages 26–33 years, mean 29) were studied. Informed consent was obtained prior to the study. Brief electrical stimuli with 0.2 ms duration were delivered to the right median nerve at the wrist (cathode proximal) with a repetition rate of 4 Hz. The stimulus intensity was three times sensory threshold and elicited a mild twitch of the abductor pollicis brevis muscle. Magnetic recordings (bandpass 0.1–1200 Hz) were taken from the left hemisphere centering at C3 of the international 10-20 system with a 37-channel SQUID gradiometer (BTi Magnes, San Diego, CA) in a magnetically shielded room. The detection coils of the gradiometer are arranged in a uniform, concentric array on a spherical surface with a radius of 122 mm; each coil measures 20 mm in diameter. The sensors are configured as first-order axial gradiometers with a baseline of 50 mm. The field sensitivities of the sensors were $10\,\mathrm{fT}/\sqrt{\mathrm{Hz}}$ or better. An epoch of 50 ms duration (10 ms pre- and 40 ms post-stimulus) was digitized at a 4000 Hz/channel sampling rate and 4000 responses were averaged off-line. DC offset was based on the pre-stimulus period.

The origin of the head-based co-ordinate system was defined as the midpoint between the pre-auricular points. The x-axis pointed from the origin to the nasion, the y-axis to the left pre-auricular point, and the z-axis to the vertex in a direction perpendicular to the x–y plane. Magnetic resonance imaging (MRI) was acquired with spherical lipid markers (5 mm diameter) placed on the MEG fiduciary points to allow for superposition of source locations onto the MRI slices. A local spherical model was fitted to the digitized head shape over the recording area for each subject.

Data analysis: The MEG vector beamformer technique was applied to localize sources from the N20m-P22m component. The results of the analysis were shown as current–density maps for transverse, coronal and sagittal sections of the generic head. Furthermore, the locations of the highest intensities of the current sources in the two activation areas (areas 1 and 3b) were overlaid on the MRI slices. The details of this vector beamformer technique have been reported elsewhere [9,10], so it is only briefly described here.

Let us define the magnetic field measured by the mth sensor at time t as $b_m(t)$, and a column vector $\mathbf{b}(t)=[b_1(t),...,b_m(t)]^{\mathrm{T}}$ as a set of measured data. Here M is the total number of sensors and the superscript T indicates the matrix transpose. A spatial location (x,y,z) is represented by a three-dimensional vector $\mathbf{r}$: $\mathbf{r}=(x,y,z)$ The source moment magnitude at $\mathbf{r}$ and time t is defined as a three-dimensional vector $\mathbf{s}(\mathbf{r},t)=[s_x(\mathbf{r},t),s_y(\mathbf{r},t),s_z(\mathbf{r},t)]$. The estimate of the source moment is denoted as $\hat{\mathbf{s}}(\mathbf{r},t)$. We define $l^x{}_j(\mathbf{r})$, $l^y{}_j(\mathbf{r})$ and $1^z{}_j(\mathbf{r})$ as the jth sensor output when a single source exists at $\mathbf{r}$ with the unit moment directed in the x, y, and z directions, respectively. We then define the lead field matrix $\mathbf{L}(\mathbf{r})$ as a matrix whose jth row is equal to $[l^x{}_j(\mathbf{r}),l^y{}_j(\mathbf{r}),l^z{}_j(\mathbf{r})]$; this lead field matrix represents the sensitivity of the whole sensor array at $\mathbf{r}$.

The vector beamformer technique reconstructs the source moment by applying the following linear operation:

$$\hat{\mathbf{s}}(\mathbf{r},t) = \mathbf{W}^{\mathrm{T}}(\mathbf{r})\mathbf{b}(t) \tag{1}$$

where the matrix $\mathbf{W}(\mathbf{r})$ is a weight matrix defined as $\mathbf{W}(\mathbf{r})=[\mathbf{w}_x(\mathbf{r}),\mathbf{w}_y(\mathbf{r}),\mathbf{w}_z(\mathbf{r})]$, and the weight vectors $\mathbf{w}_x(\mathbf{r}),\mathbf{w}_y(\mathbf{r})$ and $\mathbf{w}_z(\mathbf{r})$ detect the x, y, and z components of the source moment, respectively. Let us define the measurement covariance matrix as $\mathbf{D}$, and define the three-dimensional unit column vector as $\mathbf{f}_x$, $\mathbf{f}_y$, and $\mathbf{f}_z$. The weight vectors in an intermediate stage are first obtained using

$$\overline{\mathbf{w}}_\mu(\mathbf{r}) = \mathbf{D}^{-1}\mathbf{L}(\mathbf{r})[\mathbf{L}^{\mathrm{T}}(\mathbf{r})\mathbf{D}^{-1}\mathbf{L}(\mathbf{r})]\mathbf{f}_\mu/\sqrt{\mathbf{f}^{\mathrm{T}}{}_\mu\Omega\mathbf{f}_\mu}$$

where $\mu=$ x, y, or z, and

$$\Omega = [\mathbf{L}^{\mathrm{T}}(\mathbf{r})\mathbf{D}^{-1}\mathbf{L}(\mathbf{r})]^{-1}\mathbf{L}^{\mathrm{T}}(\mathbf{r})\mathbf{D}^2\mathbf{L}(\mathbf{r})[\mathbf{L}^{\mathrm{T}}(\mathbf{r})\mathbf{D}^{-1}\mathbf{L}(\mathbf{r})]^{-1} \tag{2}$$

Let us define $\mathbf{E}_s$ as a matrix whose columns consist of the signal-level eigenvectors of $\mathbf{D}$. Then, the final form of the weight vectors are obtained by projecting the weight vector $\overline{\mathbf{w}}_\mu$ onto the signal subspace of the measurement covariance matrix, i.e.

$$\mathbf{w}_\mu(\mathbf{r}) = \mathbf{E}_s\mathbf{E}^{\mathrm{T}}{}_s\overline{\mathbf{w}}_\mu(\mathbf{r}). \tag{3}$$

Then the source moment at $\mathbf{r}$ is estimated using Eqn (1) with the weight vectors obtained using Eqns (2) and (3). Note that when calculating the above weight vectors, the location $\mathbf{r}$ is a controllable parameter. Therefore, the source-moment distribution can be reconstructed by scanning the beamformer output over the region of interest in a completely post-processing manner. Because this reconstruction is performed at each instant in time, the spatio-temporal reconstruction of the source activities can be obtained.

RESULTS

The top traces in Fig. 1 illustrate N20m-P22m response in an extended time scale recorded over hand SI in the left hemisphere. The magnetic signals start 15 ms after right median nerve stimulation. The N20m peak occurs at 18.5 ms. The current–density maps produced by application of the beamformer technique to the MEG data revealed initial activation in area 3b of SI hand area at 17.4 ms (a selected sampled point shown by a red dotted line on the superimposed SEF traces). Other sampled points in the SEFs were indicated by green (18.5 ms), blue (19.6 ms) and black (21.1 ms) dotted lines (Fig. 1). These maps clearly show that the first source moves serially toward lateral and inferior direction around the peak of N20m (compare the maps at 17.4 ms post-stimulus in the top row and those at 18.5 ms and at 19.6 ms in the second and third rows). Just before termination of the movement

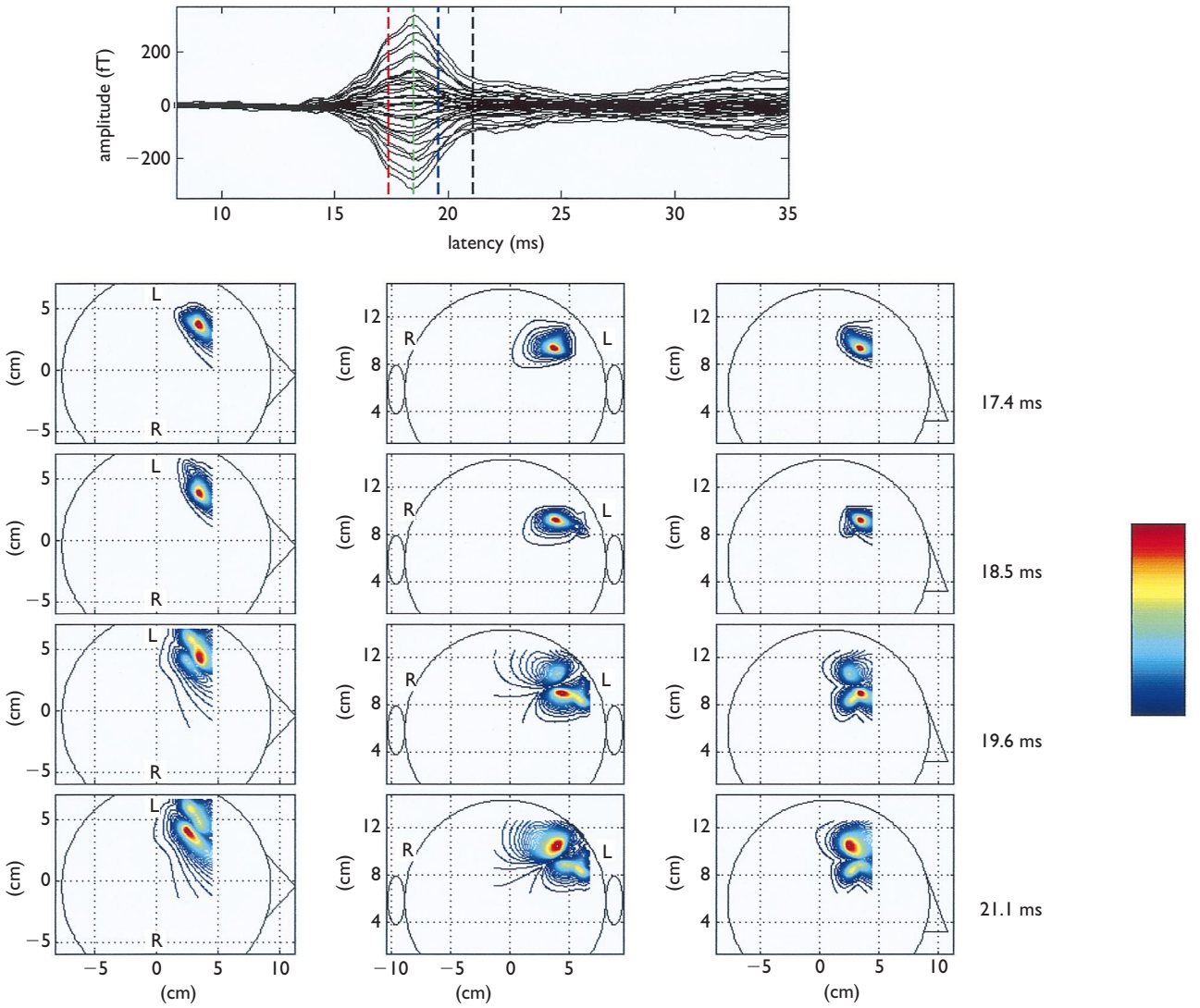

Fig. 1. Current-density maps at selected time points during N20m response. The top traces show N20m response recorded over hand S1 in the left hemisphere after median nerve stimulation. The contour maps show reconstructed source magnitude distributions at four different latencies. The maximum-intensity projections onto the axial (left column), coronal (middle column), and sagittal (right column) directions are shown. The letters L and R in the coronal views indicate the left and right hemispheres, respectively. The circles depicting a human head show the projections of the sphere used for the forward modeling. The colors of contours represent the relative intensity of the source magnitude; the relationship between the colors and relative intensities is indicated by the color bar. The maps illustrate that the first source moves sequentially toward lateral direction around the peak of N20m. Near the end of the movement of the first source, the second source located postero-medial to the first source begins to be active. The second source is stationary throughout its activation.

of the first source in the area 3b, the second source in an area posterior-medial to the first source became active (19.6 ms). In sharp contrast with the first source, the second source was stationary throughout N20m-P22m response and only the signal strength increased until the peak of P22m. However, in this subject, there was no P22m distinct from this underlying N20m and thus the primary response was single peaked. Nevertheless, the second source, clearly separated from the first source, was detected (21.1 ms). The first source began to disappear at the peak of the second source. Figure 2 shows the results of co-registration of two MEG sources of area 3b and area 1 onto the subject MRI.

The temporal and spatial relations between the two sources were summarized in Table 1, Table 2 and Table 3. In order to facilitate comparison between individual subjects with different lengths of conduction pathways, the time origin was set at the peak of N20m (Table 1). Similarly, the spatial origin was set at the location of the first source at the peak of N20m with the highest current-source density (Table 1, Table 2). With these normalization processes interindividual anatomical variations documented for the central sulcus with respect to the head coordinate system can be minimized. The latency of N20m peak ranged between 17.5 ms and 20.9 ms with the mean of 18.4 ms after median nerve stimulation (Table 1). The shortest latency when the first source started to move toward lateral direction was 2.1 ms prior to the N20m peak and the longest latency was 0.2 ms after the N20m peak

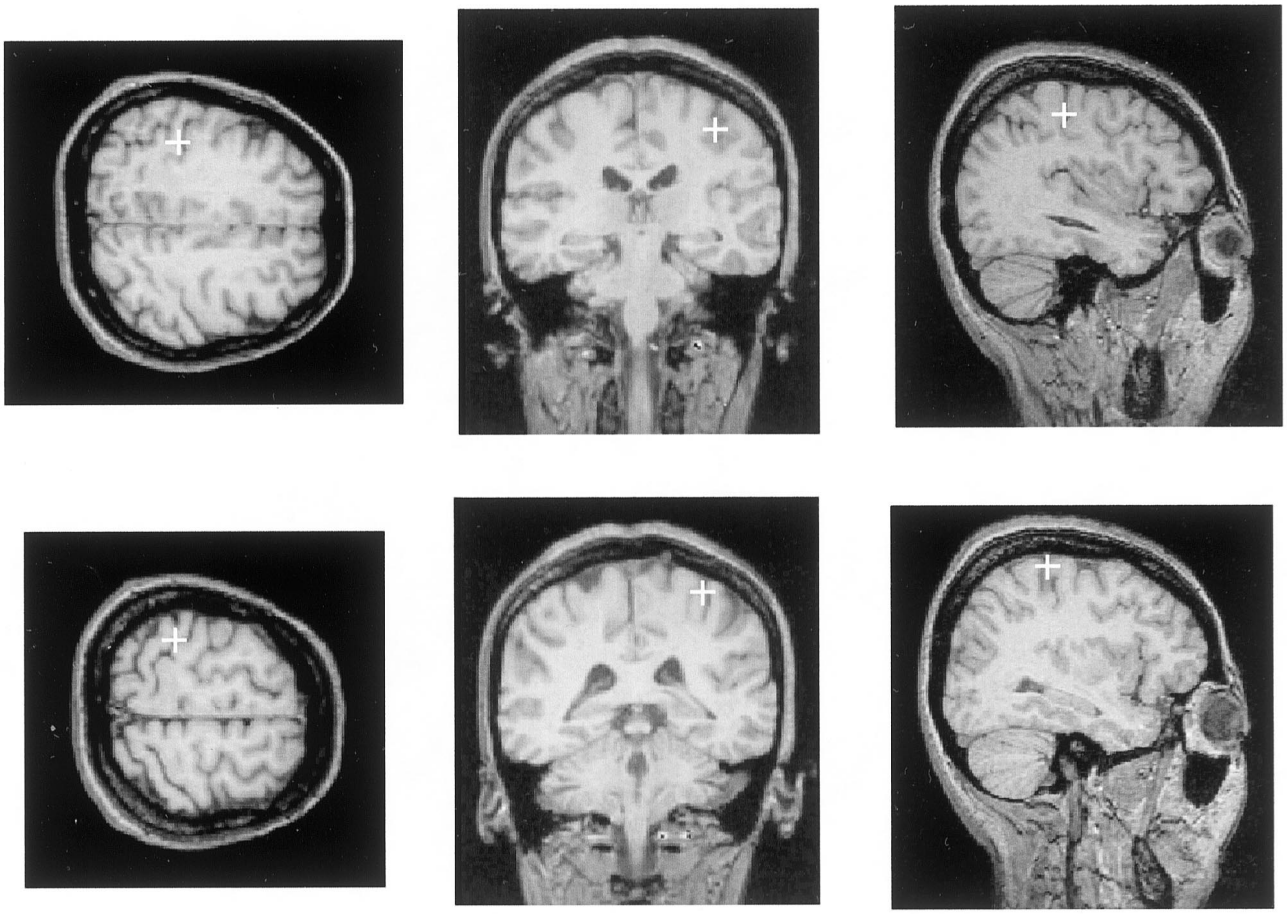

Fig. 2. Locations of the first and second sources superimposed on the axial (left), coronal (middle) and sagittal (right) sections of the subject's MRI. The location of the first source is shown in the upper images, and the location of the second source is shown in the lower images. The location of the first source is represented by that of the source at the peak vertex of N20m.

Table 1. Latencies (ms) of the first and second sources during N20m-P22m primary response[a].

Subject	N20m peak	1st source movement starts	1st source movement finishes	2nd source turns on
1	18.00	−0.70	0.70	0.24
2	17.50	−1.20	1.40	0.74
3	18.50	−0.26	1.18	0.94
4	17.50	−2.14	0.50	0.00
5	20.90	0.20	3.10	2.80
6	18.00	−0.20	1.20	0.96
Mean	18.40	−0.72	1.35	0.95
s.d	1.28	0.85	0.92	0.99

[a]Values normalized with respect to the peak latrencies of N20m.

with the mean of 0.7 ms before the peak. Similarly, the latency when the movement of the first source terminated ranged from 0.5 ms to 3.1 ms after the N20m peak with the mean of 1.4 ms post-peak. The second source started to appear between 0 ms (the peak of N20m) and 2.8 ms post-peak with the mean of 1.0 ms following the N20m peak.

The localizations of the first source at the initial and final position, and of the second source are summarized in Table 2. The first source at the initial position was located close to the original position. There was a robust trend for the initial activation to move sequentially toward lateral and inferior direction in area 3b with the mean final position at 6.4 mm lateral and 5.2 mm inferior from the original position. This was followed by activation in area 1: 4.2 mm posterior, 5.6 mm medial and 8.0 mm higher to the initial activation at the peak of N20m. ANOVA showed statistical significance for each coordinate for the three positions and the difference was significant for all coordi-

Table 2. Localization of the first and second sources during N20m-P22m response[a].

Subject	First initial (A)			First final (B)			Second (C)		
	x1	y1	z1	x2	y2	z2	x3	y3	z3
1	−2.5	−5.0	−2.1	2.1	5.0	1.3	−9.2	−7.6	22.0
2	0	0.8	1.7	3.4	10.0	−14.7	0.4	−0.4	2.0
3	−0.4	−0.8	0	0	5.0	−2.5	−9.2	2.1	11.7
4	−3.4	3.4	4.2	0	0.8	−0.8	−0.3	−16.0	13.0
5	−0.4	0	0	1.7	3.4	−4.2	−4.6	−11.0	−2.5
6	0	0	0.8	0.8	14.0	−10.0	0.4	−0.8	2.0
Mean	−1.1[b]	−0.3[c]	0.8[d]	1.3	6.4	−5.2	−4.2[e]	−5.6[f]	8.0[g]
s.d.	1.5	2.7	2.1	1.3	4.8	6.1	4.3	7.1	9.1

[a]The values were normalized with respect to those for the first source at the peak of N20m, and the values are expressed in mm.
ANOVA for [b]x ($p = 0.012$), [c]y ($p = 0.004$) and [d]z ($p = 0.10$) coordinate. Multiple comparison was assessed using Scheffé's test: significance between B and C at [e]$p = 0.012$, [f]$p = 0.004$ and [g]$p = 0.010$ for x, y and z coordinates, respectively.

Table 3. Distances (mm) from the origin (location of the first source at the peak of N20m) to the second source (0-C) and among the first source at the initial (A) and final (B) position, and the second source (C)[a].

Subject	A-B	B-C	A-C	0-C
1	11.5	26.7	25.1	25.0
2	19.1	19.9	1.3	15.0
3	6.3	17.2	14.9	15.0
4	6.6	21.9	21.3	20.8
5.	5.8	15.8	12.0	12.2
6.	17.7	19.1	1.5	2.2
Mean[b]	11.2	20.1	12.7	12.9
s.d.	6.0	3.9	9.9	9.5

[a]The distance of A-B, for example, is defined as $\sqrt{(x1-x2)^2 + (y1-y2)^2 + (z1-z2)^2}$ in Table 2.
[b]ANOVA, $p = 0.096$ (not significant).

nates between the first source at the final position and the second source (Table 2). The distances between the initial and final locations of the first source distributed from 5.8 mm to 19.1 mm with the mean of 11.2 mm (Table 3). The mean total distance between the first source at the N20m peak and the second source was 12.9 mm. Comparison between the first source at the initial location and the second source revealed a similar distance (12.7 mm). Although ANOVA showed no statistical significance, the distance between the first source at the final position and the second source (20.1 mm) was longer.

DISCUSSION

The present study demonstrates that the two sources are active during the N20m-P22m response to median nerve stimulation. The first source moved from medial to lateral direction in area 3b around the peak of N20m. The finding supports our previous study showing a robust movement toward the same direction using a single moving ECD model [1]. This ECD movement was further confirmed by SEF recordings to stimulation of the index finger [11], ruling out the possible sequential activation of thalamocortical projection fibers from the ring, middle and index fingers, to thumb all innervated by the median nerve [2]. Another possibility is that the movement of the source reflects sequential activation of different projection areas by the thalamocortical afferents with different conduction velocities. Again, there have been no published data to suggest that the thalamocortical afferents project to different regions of area 3b in accordance with the different diameters of the thalamocortical fibers.

A movement of a single source such as observed in our reconstruction has been often interpreted as a result of activity of two fixed sources. This is because when we apply the single-dipole search to the magnetic field generated from two sequentially active fixed sources, the single-dipole method sometimes gives a false solution where a single source seems to move according to the phase of activation of the two sources. That is, this spurious source movement is caused by a wrong source model, i.e., by attempting to fit a magnetic field generated from a single source to that from two sources. Moreover, the chances of this movement seem to be slim, because the goodness-of-fit will necessarily be worse if two source are approximated by a single source. Our beamformer method, however, can provide the reconstruction of neural source activities without using any explicit source model. Therefore, it is not likely that the method provides a false reconstruction of a moving single source when sequentially active two fixed sources exist. Taken together, it is highly probable that the movement reflects a real activation pattern of pyramidal cells in area 3b. We suggest that the sequential mediolateral activation of the pyramidal cells in area 3b is mediated by horizontal connections cunning parallel to the cortical surface [1,11].

The P37m component after posterior tibial nerve stimulation is the primary cortical response, consisting of two components. The first source is located in area 3b in the mesial wall of the hemisphere and the second source is 12.5 mm posterior to the first source, presumably in area 1 [12]. The first source begins to be active during the initial slope of the P37m and the second source is active after the peak of P37m. The first source is analogous to the N20m for median nerve stimulation [13]. It is likely that the second source corresponds to P22m on the basis of similar spatial and temporal features [14]. However, in the majority of cases, the first source of P37m is stationary in sharp contrast with the moving source of N20m. It may be argued that this simply reflects the size of the projection area from the hand and foot; the foot area is much smaller than the hand area [15], making it difficult to detect the movement of the source, if present. In fact, P37 amplitude

of the posterior tibial nerve SEPs and SEFs is much smaller than N20 amplitude for median nerve stimulation [13,14,16,17].

Fine coordination of hand movement is accomplished by a sensorimotor integration. The cortical efferent zones in MI receive sensory information from the skin of the limb that is close to the muscle to which they project [18,19]. This sensory feedback inputs were fed into area 4 in M1 via areas 3b and 1 and played a role in monitoring of ongoing hand movements [20,21]. However, the activity of area 4 was not observed during N20m-P22m primary response in the present study. This is either due firstly to cancellation of two anti-parallel dipoles located very close with each other, one in area 3b and another in area 4, or secondly to temporal dispersion of activity as a result of an extra synaptic transmission in areas 3b and 1, or both.

It is obvious that hand movements are more complex than foot movements. The human hand has uniquely evolved functionally and morphologically [22–24]. It seems reasonable to expect that the human brain has also evolved in relation to the important roles played by the human hand, and that somatosensory information from the hand would be processed adaptably for a fine motor control of the hand. We speculate that the dynamic movement of the first source in the median nerve SEFs reflects integration of the somatosensory information from the hand, which has been first preprocessed by the columnar organization with vertical, translaminar connectivity of intrinsic circuitry [25]. This integration is mediated by horizontal fibers connecting nearby columns and these intracortical connections could form the basis of convergence in spatial as well as non-spatial information at an early stage of somatosensory information processing [26].

Most pyramidal cells in layer 3 have 1–3 major collaterals with long horizontal trajectories (6 mm or more) in layers 3 and 4 [27–29]. Indeed, the horizontal intracortical connection is the principal route for horizontal spread of excitation in neocortex [26,30]. In monkey somatosensory cortex, it has been shown that the metabolic labeling patterns with 2-deoxyglucose to stimulation of a single finger are spatially extensive and complex [31,32]. The prominent characteristic of the distribution is a focal patch near the 3b-1 border in the most medial sections with multiple patches extending 4 mm in length from posteromedial to anterolateral direction in area 3b. The mediolateral extent of somatosensory cortex is about 3.5 cm in monkeys and about 10 cm in humans [2]. Assuming a similar projection of the body surface onto area 3b in both species, the estimated distance between the most medial and lateral activation in humans would be 11.4 mm, very similar to the average distance (11.2 mm) between the initial and final location of the moving source in area 3b in the present study or in the previous studies (8.4–8.7 mm) using a single dipole model [1,11]. However, the metabolic labeling patterns can offer no clue on the timing of activation of each patch. Thus, our previous and the present studies are the first to demonstrate a dynamic sequence of activation of the area 3b unavailable with metabolic or intracranial SEP studies.

Near the end of the first source movement, the second source, located medial and posterior to the first source in area 1, begins to be active. The second source is characterized by the steady, fixed position throughout its activation period. The different behavior of the two sources (moving *vs* stationary) suggests that P22 reflects activation of area 1 through parallel inputs from the thalamus and not through serial inputs from area 3b. It is rather surprising that the second source in area 1 was visualized in all the subjects examined, because P22 component of SEPs has been considered to reflect the radial current flow and MEG is blind to radial sources. The findings suggest that, although the currents are mainly radial, there is also a robust tangential component in P22 as reflected in P22m [3,4]. It is likely that the anterior part of area 1 within the central sulcus or at the border between the sulcus and the gyrus may be the generator of P22m. The distance between the first source at the peak of N20m and the second source (the mean of 12.9 mm) is similar to the distance measured in intracranial surface recordings of SEPs in which P22 with the largest amplitude on the postcentral gyrus (area 1) is located 1 cm medial to the focus of N20 component [2]. The time courses of activation of the first and second sources are also in line with those in cortical SEP recordings [2].

However, the cortical SEP recordings failed to detect the robust serial movement of the first source in area 3b demonstrated by magnetic recordings. In the study of Allison *et al*. [2], cortical SEPs were usually recorded from a 64-electrode array (8×8 grid) with 5 mm interelectrode spacing. Provided that the moving source is directly under the electrodes, this electrode density will give nearly optimal spatial resolution of voltage gradient of the currents for the first source. However, area 3b lies within the central sulcus, the depth of which ranges from 16 to 18 mm [33,34] to 20 mm [35], making direct recordings of activity in area 3b difficult with the surface electrode array over the gyri near the central sulcus. It is likely that, in this situation, extracellular volume currents are recorded more or less as far-fields and not as near-fields even in cortical recordings, resulting in smearing of spatial resolution (see [2,36] for intracranial distribution of auditory and somatosensory evoked potentials).

Thus, the discrepancy between the cortical EEG recordings and the magnetic recordings outside the head is one excellent example of the advantages of MEG over EEG. This is mainly due to the fact that, first, the tissues inside and outside the brain do not significantly distort the magnetic field patterns generated by brain currents and recorded outside the head. Secondly, MEG source localization is better in the direction orthogonal to the dipole orientation [37] and the movement of the first source is orthogonal to the N20m ECD orientation [1,11]. This poses a serious question, because interpretation of MEG data has been heavily dependent on direct cortical recordings of the electric counterpart for the MEG signals, which have been considered to provide a 'gold standard' for 'real' brain activation. Conversely, it is possible that MEG recordings may, in favorable conditions, provide a touchstone leading to new findings in the physiological activity of the human brain non-invasively.

CONCLUSION

The MEG vector beamformer technique visualized non-invasively a serial mediolateral activation of the human somatosensory 3b area followed by a stationary activation

of area 1 after median nerve stimulation. The first source located in area 3b started to move sequentially toward mediolateral direction prior to the peak of N20m. We speculate that the movement reflects a sequential activation of the pyramidal cells in area 3b, which is mediated by horizontal connections running parallel to the cortical surface [1,11]. The second source in area 1, located medial and posterior to the first source, was active after the N20m peak. In sharp contrast with the first source, the second source was stationary, suggesting independent parallel inputs to area 3b and area 1 from the thalamus.

REFERENCES

1. Hashimoto I, Kimura T, Sakuma K *et al*. *Neurosci Lett* **280**, 25–28 (2000).
2. Allison T, McCarthy Q Wood CC *et al*. *J Neurophysiol* **62**, 694–710 (1989).
3. Tiihonen J, Hari R and Hamalainen M. *Electroencephalogr Clin Neurophysiol* **74**, 290–296 (1989).
4. Kakigi R. *Neurosci Res* **20**, 165–174 (1994).
5. Buchner H, Waberski TD, Fuchs M *et al*. *Electroencephalogr Clin Neurophysiol* **100**, 332–342 (1996).
6. Yumoto M, Uesaka Y, Ugawa Y *et al*. Localization of somatosensory evoked P22 component by magnetoencephalography. In: Hashimoto I, Okada Y and Ogawa S, eds. *Visualization of Information Processing in the Human Brain: Recent Advances in MEG and Functional MRI* (EEG Suppl. 47). Amsterdam, Elsevier, 1996: 97–101.
7. Yousry TA, Schmid UD, Alkadhi H *et al*. *Brain* **120**, 141–157 (1997).
8. Huttunen J. *Electroencephalogr Clin Neurophysiol* **104**, 101–102 (1997).
9. Sekihara K, Nagarajan SS, Poeppel D *et al*. *NeuroImage* **11**, 485 (2000).
10. Sekihara K, Nagarajan SS, Poeppel D *et al*. *IEEE Trans Biomed Eng* (in press).
11. Kimura T and Hashimoto I. *Neurosci Lett* **297**, 61–64 (2001).
12. Hashimoto I, Sakuma K, Kimura T *et al*. *Neuroreport* **12**, 1857–1862 (2001).
13. Hari R, Nagamine T, Nishitani N *et al*. *NeuroImage* **4**, 111–118 (1996).
14. Kakigi R, Koyama S. Hoshiyama M *et al*. *Electroencephalogr Clin Neurophysiol* **95**, 134 (1995).
15. Penfield W and Boldrey E. *Brain* **60**, 389–443 (1937).
16. Nakano S and Hashimoto I. *Electroencephalogr Clin Neurophysiol* **110**, 1948–1952 (1999).
17. Sakuma K and Hashimoto I. *NeuroReport* **10**, 227–230 (1999).
18. Asanuma H and Rosen I. *Exp Brain Res* **14**, 243–256 (1972).
19. Rosen I and Asanuina H. *Exp Brain Res* **14**, 257–273 (1972).
20. Terao Y, Ugawa Y, Uesaka Y *et al*. *Electroencephalogr Clin Neurophysiol* **97**, 375–381 (1995).
21. Terao Y, Ugawa Y, Hanajima R *et al*. *Brain* **122**, 2256–2277 (1999).
22. Napier J. *Sci Am* **206**, 56–62 (1962).
23. Susman RL. *Science* **265**, 1570–1573 (1994).
24. Susman RL. *J Hum Evol* **35**, 23–46 (1998).
25. Mountcastle VB. *J Neurophysiol* **20**, 408–434 (1957).
26. Jones EG. *Cereb Cortex* **3**, 361–372 (1993).
27. DeFelipe J, Conley M and Jones EG. *J Neurosci* **6**, 3749–3766 (1986).
28. Gilbert CD and Wiesel TN. *J Neurosci* **9**, 2432–2442 (1989).
29. McGuire BA, Gilbert CD, Rivlin PK and Wiesel TN. *J Comp Neurol* **305**, 370–392 (1991).
30. Langdon RB and Sur M. *J Neurophysiol* **64**, 1484–1501 (1990).
31. Juliano SL and Whitsel BI. *Brain Res* **342**, 242–251 (1985).
32. Juliano SL and Whitsel BI. *J Comp Neurol* **263**, 514–525 (1987).
33. Ono M, Kubic S and Abemathey CD. *Atlas of the Cerebral Sulci*. Stuttgart: Georg Thieme Verlag; 1990.
34. Allison T, McCarthy Q Wood CC and Jones SJ. *Brain* **114**, 2465–2503 (1991).
35. Delmas A and Pertuiset B. *Cranio-Cerebral Topometry in Man*. Springfield, IL: Charles Thomas; 1959.
36. Hashimoto I. *Electroencephalogr Clin Neurophysiol* **53**, 652–657 (1982).
37. Hari R, Joutsiniemi S-L and Sarvas J. *Electroencephalogr Clin Neurophysiol* **71**, 64–72 (1988).

Acknowledgements: This research was supported by a Grant-in-Aid for Scientific Research from the Ministry of Education, Science and Culture of Japan (09877185) and a Grant-in-Aid of the Japan Medical Association (1998). One of the authors (K.S.) was supported by a research project 'Mind Articulation' sponsored by Japan Science and Technology Corporation.